Transport characteristics of Pd Schottky barrier diodes on epitaxial *n*-GaSb as determined from temperature dependent current-voltage measurements

A. Venter[1,*], D.M. Murape[1], J.R. Botha[1] and F.D. Auret[2]

[1]*Department of Physics, Nelson Mandela Metropolitan University*, *P.O. Box 77000, Port Elizabeth 6031, South Africa*

[2]*Department of Physics, University of the Pretoria, Lynnwood Road, Pretoria 0002, South Africa*

**E-mail: andre.venter@nmmu.ac.za (corresponding author)*

Tel: +27(0)415042579

Fax:+27(0)415041989

Highlights

- Transport characteristics of Pd/epitaxial *n*-GaSb:Te SBDs are studied by means of I-V-T measurements.
- SBDs have remarkably low and saturating reverse current – of the lowest ever reported for GaSb.
- Transport behaviour is explained by considering electronic states present on the GaSb surface.
- Evidence is presented for barrier inhomogeneity across the metal-semiconductor contact.

Abstract:

The temperature dependent transport characteristics of Pd/*n*-GaSb:Te (MOCVD) Schottky contacts with low and saturating reverse current are investigated by means of current-voltage (*I*-*V*) measurements between 80 K and 320 K. The apparent barrier height and ideality factor increase with decrease in temperature. Neither thermionic (TE) nor thermionic field emission (TFE) can explain the low temperature characteristics of these diodes. Instead, evidence is presented for barrier inhomogeneity across the MS contact. A plot of the barrier height, ϕ_b vs 1/2kT revealed a double Gaussian distribution for the barrier height with $\phi_{b,\mathrm{mean}}$ assuming values of 0.59 eV ± 0.07 (80-140 K) and 0.25 eV ± 0.12 (140-320 K) respectively.

Introduction

Epitaxial material systems based on gallium antimonite (GaSb) have numerous potential applications including low threshold voltage infra-red (IR) lasers, photo-detectors with high quantum efficiency, booster cells in tandem solar cell arrangements for improved efficiency, thermo-photovoltaic (TPV) cells, microwave devices, fire detection, and IR sensing for missile and surveillance systems, to mention a few. [1, 2, 3]. In addition to these, potential environmental applications include the monitoring of gas purity as well as the detection of corrosive gases such as hydrogen chloride (HCl), hydrogen fluoride (HF) and hydrogen sulphide (H_2S) “leaks” in chemical plants [1]. Despite these numerous potential applications, GaSb related technology is immature and faces a number of major challenges including chemical non-uniformity across the surface [1, 4]. For example, III/V antimonides in general have poor surface electronic properties, resulting from high surface state densities. Since semiconductor devices draw on surface and interface properties, the GaSb surface presents a major challenge to device fabrication and subsequent performance. In particular, GaSb is known to oxidise readily, resulting in the formation of a persistent native oxide layer. It is consequently characterised by a high density of surface states, some of which are acting as non-radiative recombination centres, detrimental to the development of emissions devices of high quantum efficiency. Furthermore the presence of elemental Sb on the surface creates a conduction path parallel to the active surface region, resulting in the non-ideal behaviour of GaSb-based devices [1, 5, 6]. These factors by and large restrict the potential that GaSb and GaSb-based strained layer super lattices offer as successors to the current generation of long wavelength (LWIR) and very long wavelength infra-red (VLWIR) - optoelectronic materials. Significant progress is consequently required before the potential that GaSb offers may be fully exploited.

Schottky barrier diodes (SBDs), predominantly because of its simplicity, have become indispensable in the characterisation of semiconductor materials [7, 8]. This device and related micro-electronic devices are often required to operate at extreme temperatures without sacrificing efficiency or reliability. Furthermore, the electronic properties of these devices - largely determined by the nature of the barrier formed between the metal and the semiconductor - may be better understood by studying its temperature dependent current transport. Although many reports exist on the temperature dependence of current-voltage *(I-V)* characteristics of metal semiconductor contacts (both ohmic and rectifying) on a number of semiconductors [7, 8, 9, 10, 11, 12, 13, 14], to our knowledge, very few such reports exist on GaSb and in particular, epitaxially grown GaSb thin films. Studies have shown that temperature dependent current transport (especially at low temperatures) often cannot be explained satisfactorily by thermionic emission processes alone [7, 15, 16]. Inconsistency with thermionic emission theory, even for lowly doped (10^{15} cm^{-3}) material, becomes evident upon plotting the logarithm of the saturation current divided by the square of the temperature ($ln(I_0/T^2)$) against the inverse of the temperature $(1/T)$ to which a Schottky barrier diode is exposed [12]. Typically, an increase in the ideality factor (n), accompanied by a decrease in the barrier height (ϕ_b) at low temperatures suggest non-linearity in the activation energy of the resulting Arrhenius plot. Numerous authors attribute this anomaly to a Gaussian distribution in the spatial variations in the barrier height. [8, 16, 17, 18, 19].

This work reports on the temperature dependent *I-V* behaviour of Pd SBDs fabricated on Te doped epitaxial *n*-GaSb layers in the temperature range 80 K – 320 K. Strong evidence is presented for the existence of a Gaussian distribution of barrier heights resulting from in-homogeneity of the barrier height at the MS interface.

Experimental Procedure

Epitaxial *n*-GaSb:Te layers (~3 µm thick) were simultaneously grown by metalorganic vapour phase epitaxy (MOVPE) on (100)B n^+-GaSb:Te, as well as on (100) SI GaAs, both misoriented by 2° towards the <110>. The latter was grown exclusively for the purpose of establishing the free carrier concentration of the epilayer by Hall effect measurements. Both substrates were supplied by Semiconductor Wafer Inc. The growth was performed at atmospheric pressure in a horizontal MOVPE reactor using triethylgallium (TEGa) and triethylantimony (TMSb) as precursors while diethyltellurium (DETe) was used as the doping source. The substrates were neither organically cleaned nor etched prior to growth. The free carrier concentration (N_d) of the *n*-GaSb epilayer grown on SI GaAs, determined by room temperature (RT) Hall effect measurements in the Van der Pauw configuration, was found to be 5×10^{16} cm^{-3}. Next the samples were organically cleaned by successively (×3) boiling it in trichloroethylene, acetone and methanol, followed by a quick rinse in de-ionized (DI) water (ρ = 18.2 MΩ.cm). Following this, the samples were deoxidized in 18.5 % (by volume) HCl for 30 s, blown dry with nitrogen and promptly loaded into a turbo vacuum system (base pressure = 5×10^{-5}Torr). Circular Pd Schottky contacts (ϕ = 0.5 mm), 100 nm thick, were subsequently resistively evaporated through a metal shadow mask. Ohmic contact to the sample was achieved by rubbing liquid gallium indium (GaIn) eutectic on the back surface of the n/n$^+$ structure. Temperature dependent *I-V* measurements were performed between 80 and 320 K using an automated HP 4140B DC voltage source / pA current meter system interfaced with a PC and a specially designed sample mounting system fitted with a foil heater and a Si diode temperature sensor. Low temperatures were achieved by keeping the sample just above liquid nitrogen and the heater was used to attain equilibrium through a LakeShore 330 auto-tuning temperature controller. Temperature fluctuations were maintained within ±0.5 K during data acquisition.

Results and Discussion

According to current transport theory, the dominant mechanism associated with a SBD, may be determined by calculating a tunnelling parameter for the structure. The tunnelling parameter E_{00} is given by the following expression [20, 21]:

$$E_{00} = {}^{qh}/_{4\pi} \left({}^{N_d}/_{m^* \varepsilon_s} \right)^{1/2} \tag{1}$$

where N_d is the free carrier concentration at the metal semiconductor interface, m* is the tunnelling effective mass and ε_s, the dielectric constant of GaSb. Clearly the tunnelling parameter is proportional to $\sqrt{N_d}$. Degenerate materials are consequently expected to have highly penetrable (narrow) barriers. Typically, field emission (FE) is dominant when $E_{00} \gg kT$, thermionic field emission (TFE) when $E_{00} \approx kT$ and thermionic emission (TE) when $E_{00} \ll kT$. It is instructive to note that the ideality factor n is a measure of the degree to which the current transport in a SBD is described exclusively by TE. An ideality factor of 1 consequently reflects pure thermionic emission. Should the transport mechanism be more complex and involve both TE and TFE (or other mechanisms), the ideality factor is adjusted to account for tunnelling as described by equation 1, leading to the following equation [22, 23]:

$$n_{tun} = \left({}^{qE_{00}}/_{kT} \right) coth \left({}^{qE_{00}}/_{kT} \right) \tag{2}$$

The symbols have their usual meaning. Comparing n_{tun} with the experimentally determined ideality factor - using the slope of the linear section of the logarithm of the current plotted against the diode potential, suggests complex current transport. Figure 1 depicts E_{00}/kT values as function of temperature (open circles) together with a comparison of values for the theoretically (eq 2. - open squares) and experimentally determined (solid squares) temperature dependent ideality factor.

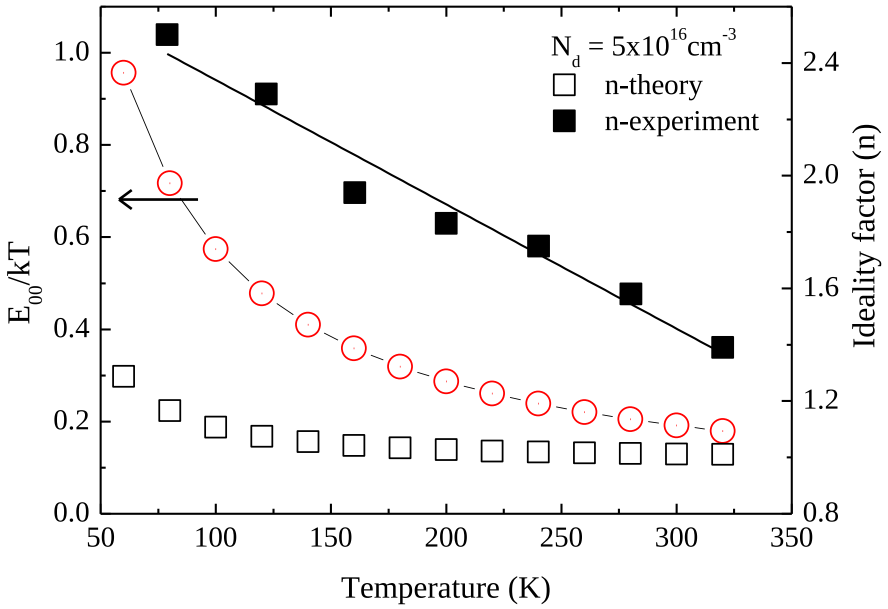

Fig. 1. E_{00}/kT values as function of temperature (open circles) and a comparison between the theoretically determined (assuming TFE - open squares) and experimentally obtained (solid squares) ideality factors.

Considering the E_{00}/kT values in Fig. 1, it is reasonable to assume that both TE and TFE or even more complicated mechanisms should be at play in the temperature range investigated (80-320 K). The current in a forward biased SBD, considering thermionic emission as the dominant charge transport mechanism is given by [24, 25, 26]:

$$I = I_s\left(exp\left(\frac{q(V-IR_s)}{nkT}\right)\right), \tag{3}$$

where IR_s is the voltage drop across the device due to its bulk series resistance. The saturation current may be expressed by [27, 28]:

$$I_s = AA^*T^2\left(exp^{-\left(\frac{q\phi_b}{kT}\right)}\right) \tag{4}$$

where A is the diode area and A^* the Richardson constant. Linearizing this equation allows the effective barrier height and the Richardson constant to be extracted. Should the transport be dominated by TFE, the saturation current density is expressed by [29]:

$$I_s = AA^* \sqrt{\pi E_{00}(\phi_b - V + \xi)}/kT coth\left(\frac{E_{00}}{kT}\right) exp\left(\frac{\xi}{kT} - \frac{\phi_b + \xi}{E_0}\right) \tag{5}$$

where $\xi = {kT}/{q}\, ln\left({N_c}/{N_d}\right)$ is the Fermi-energy relative to the bottom of the conduction band. The tunnelling factor in the above equation is given by [20]:

$$E_0 = E_{00} coth\left(\frac{E_{00}}{kT}\right) \tag{6}$$

Current –Voltage measurements

Figure 2 shows typical semi-logarithmic *I-V* characteristics of the Pd/*n*-GaSb SBD investigated between 80 K and 320 K. It is clear that the transport characteristics are complex (see encircled regions) and cannot be explained by a single transport mechanism. For the ensuing analysis, it was assumed that current transport across the barrier was mainly due to TE. The barrier height and the corresponding ideality factor at each temperature were determined using the slope and the intercept respectively of the linear portion of the *ln I* versus *V* plots. Deviation from TE was then accounted for by considering TFE instead.

Consider the reverse bias region in Fig. 2. It is clear from the gradual decrease in the reverse current with decreasing temperature that the transport properties are strongly influenced by the temperature. This behaviour is attributed to the reduced thermal energy of the system with temperature. Notably, reports on similar device structures, without exception, suggest severe non-saturating reverse current behaviour. The excessive leakage, typically ascribed to quantum mechanical (QM) or trap assisted tunnelling, is largely eliminated in this diode. The non-saturating behaviour observed at 160K and lower, suggests that field enhanced or trap-assisted tunnelling starts contributing to the current at reverse voltages exceeding roughly 250 mV. As far as could be established, the nearly saturating reverse current (up to -1V) shown in Fig. 2, represents the lowest of recent reports for a metal-semiconductor diode structure on *n*-GaSb.

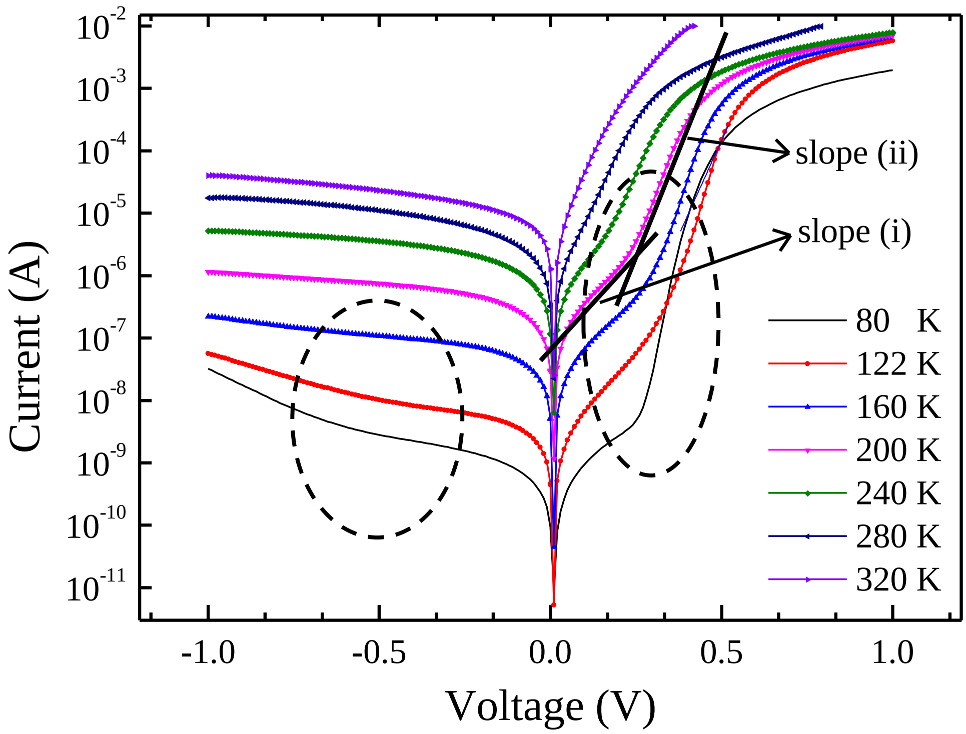

Fig.2. Current-voltage characteristics of a Pd/*n*-GaSb Schottky contact in the temperature range 80-320 K.

Next, the forward bias region is considered. At 280 K the *I-V* curve exhibit linearity over almost three orders of magnitude (on the current scale), followed by downward bending due to the series resistance *(R_s)* of the interface together with that of the GaSb epilayer. [8, 18]. Importantly, a previous study confirmed that the substantial series resistance in this case is not related the quality of the liquid GaIn eutectic ohmic contact [30]. The flattening off here is consequently ascribed to the resistance due to interface states, together with that of the GaSb epilayer. Table 1 lists the series resistance as function of temperature. The increase in series resistance with temperature is mainly attributed to a decrease in the free-carrier concentration of the material with temperature, as confirmed by Hall effect measurements (not shown).

As pointed out earlier, the deviation from linearity at low temperatures suggests that the current transport through the Pd/GaSb structure cannot be accounted for by a simple TE current transport mechanism and that TFE and possibly other mechanisms also need to be considered. An alternative explanation for the “complex” forward characteristics may be

Table 1 : Series resistance (**R_s**) of Pd/**n**-GaSb SBDs at various temperatures extracted from the least squares fit of d**V**/d(ln**I**) **vs. I** in the temperature range of 80–320 K. The series resistance has been determined using Cheung's method

Temperature (K)	80	100	122	160	200	240	280	320
R_s (Ω)	224.85	83.01	76.65	73.92	72.85	74.18	52.86	7.24

provided by considering "patchy" barriers i.e. regions on a SBD for which the barier height is significantly reduced. Clearly, the forward characteristics at 240K and lower are characterized by – excluding the series resistance region – essentially two regions having different slopes. At low biases (slope (i)) the current transport is dominated by TFE or generation - recombination via defects at the interface or possibly a more complex mechanisms. Slope (ii) represents the region where TE dominates.

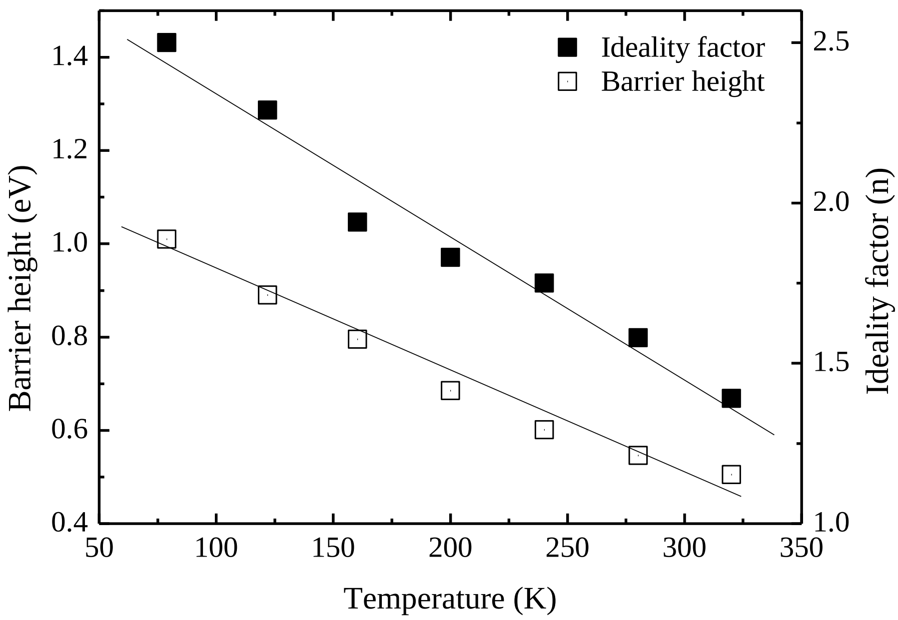

Fig. 3. Temperature dependent barrier height and ideality factor of a Pd/*n*-GaSb Schottky contact as a function of the ambient temperature. Also shown here are linear fits for the plots

Figure 3 shows the experimentally determined temperature dependent ideality factor and barrier height obtained from the *I-V* curves depicted in Figure 2. Both these parameters show inverse correlation with temperature, increasing from 0.51 eV to 1.01 eV and 1.39 to 2.5 at 320 K and 80 K, respectively. The observed increase in the zero-bias barrier height with decreasing temperature is contrary to observations for other semiconductor materials [14, 15, 18, 27, 31, 32]. Results reported in literature for similar studies on the electrical properties of GaSb rectifying structures are conflicting. Lin *et al*. [33] for example used photo-response measurement to study the temperature dependent behaviour of Au/*n*-GaSb SBDs. These authors, in agreement with our results, reported an increase in the barrier height with decrease in temperature (from 0.57 eV at 316 K to 0.69 eV at 156 K). Huang *et al*. [34] studied the temperature dependence of the *I-V* characteristics of Ni/*n*-GaSb SBDs. In their case however a decrease in barrier height from 0.49 at 373 K to 0.28 eV at 173 K was observed. The ideality factor, as is the case in this study, was found to increase with decrease in temperature. The inverse temperature dependence of the ideality factor is in agreement with that predicted by thermionic emission theory. Less thermal energy available to the MS system reduces the population of carriers with sufficient energy to scale the built-in potential, consequently reducing the thermionic current contribution to the net current crossing the junction. The increase in the barrier height to values exceeding the band gap of the material (0.73 eV at 297 K) raises an interesting point. The Fermi-level is temperature dependent and approaches the valence band edge at low temperatures [35]. The elevated barrier height is therefore possibly related to interface states, the most apparent being the persistent native oxide Ga-O detected previously by XPS [6].

Deviation from TE and TFE theory

Figure 4 depicts the tunnelling factor E_0 as function of temperature calculated using equations 3 (TE) and 6 (TFE) respectively compared to the experimental values for E_0 using the measured ideality factor. The experimentally determined tunnelling parameter clearly does not correlate with that predicted by either TE or TFE, confirming the view that a complex transport mechanism may be at play in these Pd/*n*-GaSb SBDs. Furthermore, the large difference between the experimentally obtained ideality factor (Fig. 3) and that of a SBD for which TFE is dominant (plotted in Fig. 1) can be attributed to a larger contribution (to the junction current) by carriers able to tunnel through the barrier [12, 27].

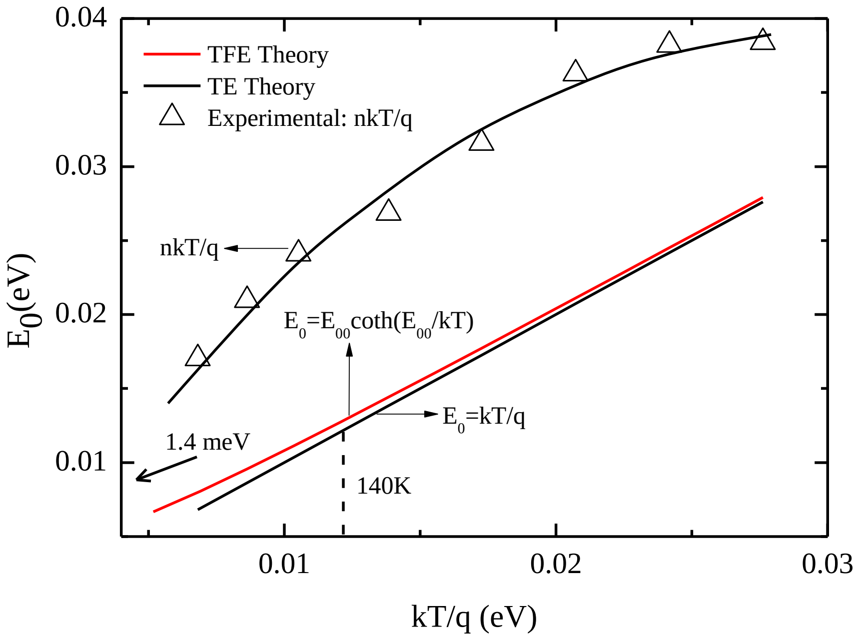

Fig. 4. E_0 as function of temperature calculated using equation 3 (TE) and 6 (TFE) respectively compared to the experimental values for E_0.

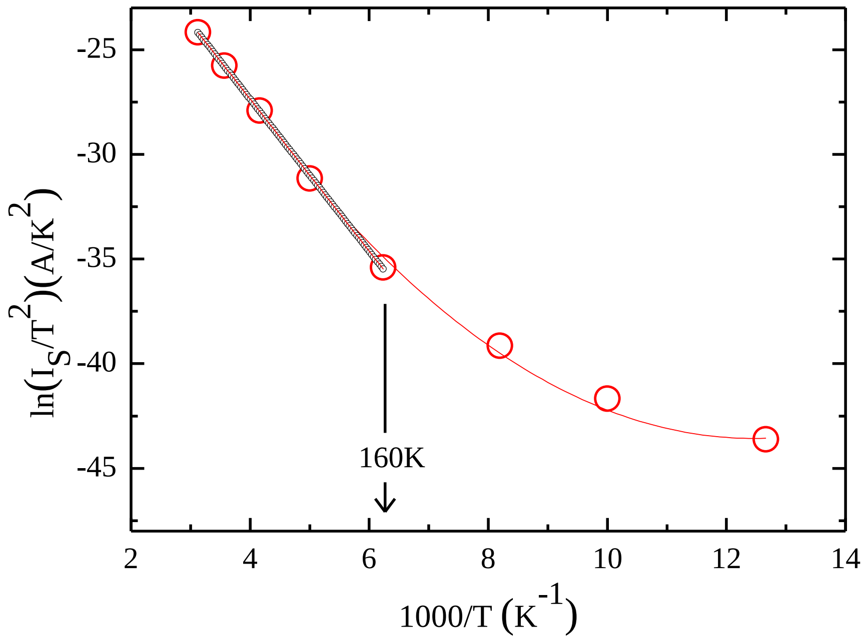

Fig. 5. A plot of the $\ln(I_s/T^2)$ versus (1000/T) for the Pd/*n*-GaSb Schottky contacts (open circles). The dotted line represents a least squares fit for the linear potion of the curve (>160 K).

Figure 5 shows a plot of $ln(I_s/T^2)\ vs\ (1000/kT)$ the so-called "conventional" Richardson plot for the Pd/*n*-GaSb SBD used in this study. Such a plot is very useful in studying the temperature dependent transport behaviour through a SBD since a linear relationship between $ln(I_s/T^2)$ and $(1000/kT)$ will confirm TE as the dominant transport mechanism. Two distinct regions are identified, the high temperature region, T > 160 K, where the relationship is clearly linear and that below 160 K showing a gradual deviation from linearity. Clearly, thermionic emission well describes the transport behaviour down to approximately 160 K but fails do so at lower temperatures. Linear fitting of the curve in the appropriate region resulted in a barrier height of 0.31 eV and a Richardson constant, A*, of 1.38 × 10^{-3} $Acm^{-2}K^{-2}$. The barrier height is significantly lower than the average value in this temperature range as is depicted in Fig. 3. The Richardson constant too is significantly lower than the accepted value of 5 $Acm^{-2}K^{-2}$ for epitaxial *n*-GaSb films [36]. Since A^* is extracted from the intercept of the Richardson plot, this large difference can partially be explained by realising that any uncertainty in the data will be exaggerated upon extrapolating $\frac{1000}{T} \rightarrow 0$. Furthermore, the increase in the ideality factor with decrease in temperature together with the low value obtained for the Richardson constant may also be evidence for an inhomogeneous Schottky barrier [37, 28]. Note that the construction of this Richardson plot in Fig. 5 is based on the assumption that the current through the device is purely due to the thermionic emission i.e. a diode for which n = 1. In practice this is not possible and to account for this, equation 3 is adjusted to accommodate for the non-ideality of the SBD:

$$I_s = AA^*T^2\left(exp^{-\left(\frac{q\Phi_b}{nkT}\right)}\right) \qquad (7)$$

Plotting $ln(I_s/T^2)\ vs\ (1000/nkT)$ should therefore result in a straight line graph. Figure 6 shows an adjusted Richardson plot. A least squares fit of the data (in the linear region) resulted in a barrier height of 0.80 eV. A crude, somewhat imaginative analysis of the data suggests a reduced barrier height with an “estimated” value of 0.26 eV in the low temperature region.

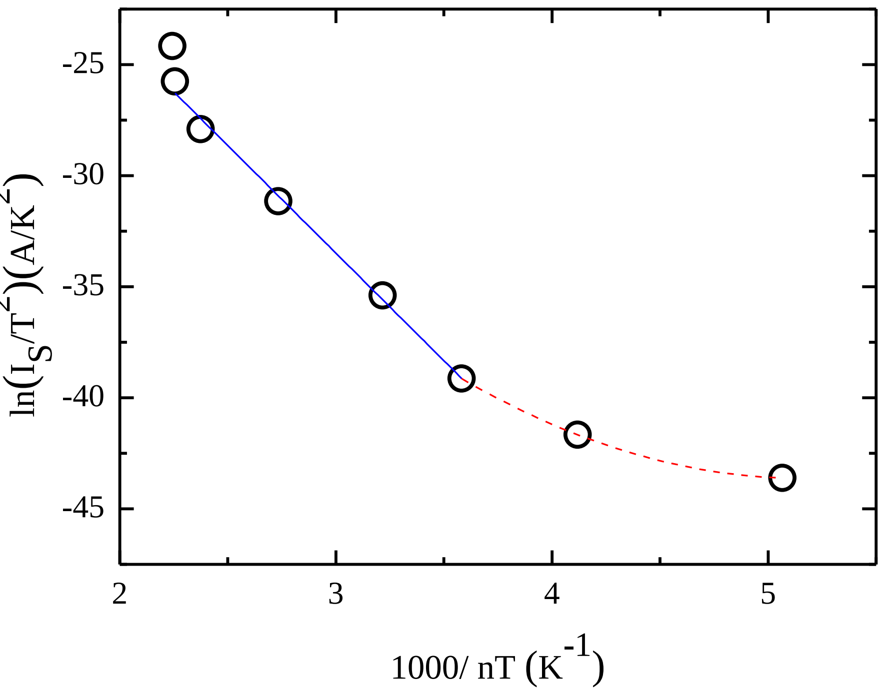

Fig. 6. An adjusted Richardson plot as expressed in equation 7. The non-ideal nature of the Pd/ *n*-GaSb SBDs has been taken into account.

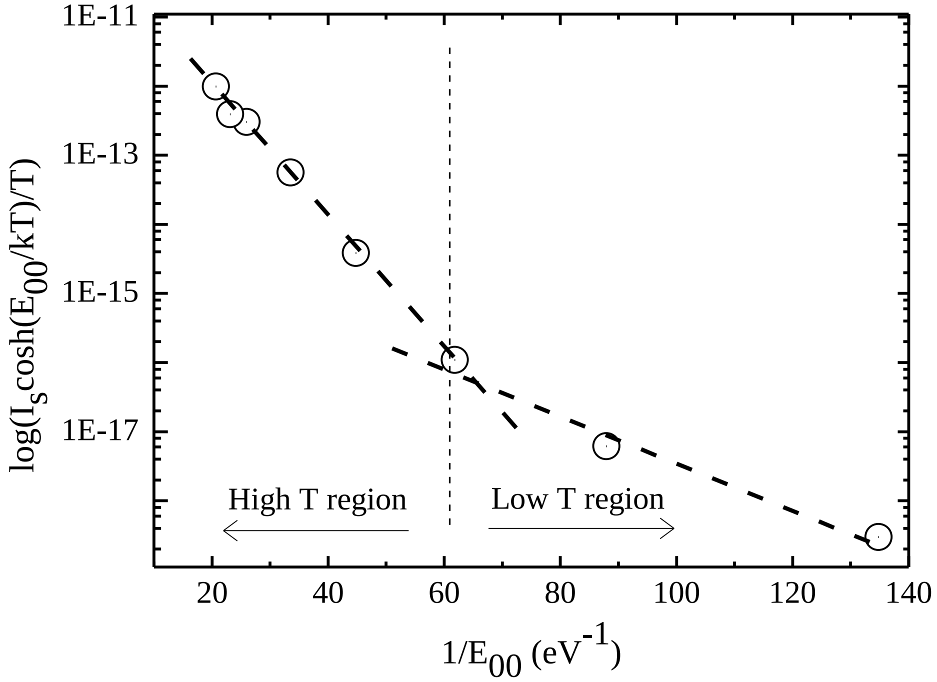

Fig. 7. The measured saturation current plotted against the tunnelling factor $1/E_0$ for the Pd/*n*-GaSb structure studied. Note the possibility of a second, much lower barrier height in the low temperature region.

Next *thermionic field emission (TFE)* theory is used to determine the temperature dependent barrier height by plotting $ln\left(\left(I_s/coth\left(\frac{E_{00}}{kT}\right)\right)/T\right)\ vs\ 1/E_0$ (rearranged from equation 5). TFE will be dominant if *this* relationship is linear. Figure 7 depicts a plot of the measured saturation current against the tunnelling factor E_0 for the Pd/*n*-GaSb structure studied. Evidently, TFE too does not account for the observed current transport behaviour. Furthermore, a second slope could possibly be associated with the low temperature region, suggesting a lower barrier height in this region. Clearly, charge transport in the Pd/*n*-GaSb structure is not simple and cannot be sufficiently explained by either *TE* or *TFE* for the entire temperature region investigated.

It is not unusual for diode parameters to vary from one contact to another even though being fabricated from the same materials and under the same experimental conditions [38]. Regarding GaSb, in a previous XPS study by ourselves [6], the persistent presence of a native oxide layer together with elemental Sb have been confirmed on the GaSb surface, despite thorough cleaning, etching and sulphur passivation. It is therefore reasonable to assume non-uniformity at the MS interface resulting in lateral inhomogeneity of the barrier height. Considering this, the barrier height may not only vary across a sample from one SBD to the

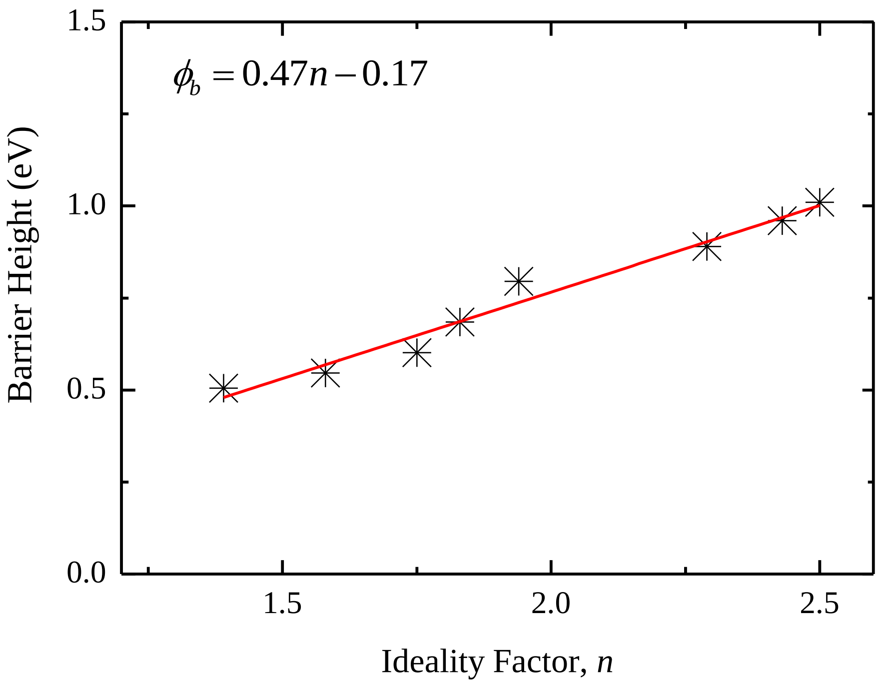

Fig. 8. Temperature dependent barrier height versus the temperature dependent ideality factor of a Pd/*n*-GaSb Schottky contact. Solid lines represent linear fits.

next (as much as 15% in this study) but also within a single SBD this may be the case. The measured barrier height (using equations 4 or 5) is consequently an average ($\phi_{b,\text{mean}}$) of a series of Gaussian distributed barrier heights characterised by a standard deviation of σ_S. This inhomogeneity may be confirmed by plotting the temperature dependent barrier height as function of the associated ideality factor and is confirmed if the relationship is linear [37, 38]. Fig. 8 shows a plot of the barrier height as function of *n(T)*. The plot exhibits linearity and therefore confirms barrier inhomogeneity in these diodes. According to the inhomogeneity model, the temperature dependence of the barrier height is defined by an average barrier height associated with a standard deviation and is expressed as follows [15, 19]:

$$\phi_b = \phi_{b\,mean} - \frac{q\sigma_S^2}{2kT} \tag{8}$$

Although σ_S is temperature dependent, the dependence is very small and usually neglected [11]. In addition to the barrier height, the “apparent" ideality factor is also temperature dependent and is expressed by [15, 19]:

$$\frac{1}{n} - 1 = -\rho_2 + \frac{q\rho_3}{2kT} \tag{9}$$

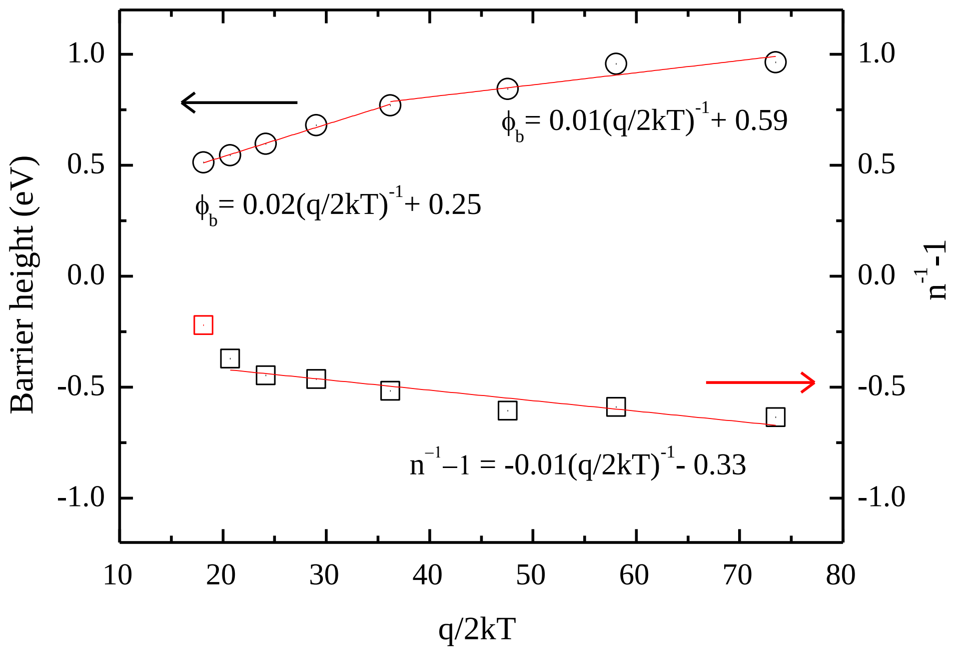

Fig. 9. The temperature dependence of the apparent barrier height and ideality factor for the Pd/*n*-GaSb structure investigated.

Here ρ_2 and ρ_3 are coefficients that describe the deformation of the spatial barrier distribution by the applied voltage. Figure 9 shows plots for ϕ_b and $\left(\frac{1}{n}-1\right)$ respectively vs q/2kT from the experimentally obtained data. Two linear regions clearly define the behaviour of the barrier height with q/2kT. In region 1, ranging from 80-140 K, we have a Gaussian distribution defined by a $\phi_{b,\mathrm{mean}}$ of 0.59 eV and a standard deviation at zero-bias of 0.07 eV. In region 2, ranging from 140-320 K, the Gaussian distribution gives a $\phi_{b,\mathrm{mean}}$ of 0.25 eV and a corresponding deviation of 0.12 eV. The possible identification of two different slopes for the ideality factor is less conspicuous. A linear fit of the data, excluding the data point at 320 K, yields a straight line in accordance with equation 9 with voltage coefficients of ρ_2 = -0.325 and ρ_3 = -0.005. This confirms the voltage deformation of the Gaussian distribution of the barrier height. We conclude that the barrier height is characterised by inhomogeneity with a double Gaussian distribution in two temperature ranges. In the lower range, i.e. 80-140 K, the mean barrier height barrier height is enhanced and has a standard deviation of around 10% while in the higher temperature range, i.e. 140-320K, the mean barrier height is 0.25 eV with a standard deviation of almost 50%.

Summary and Conclusions

The current transport of Pd/*n*-GaSb SBDs was investigated by means of *I*-*V*-*T* measurements in the temperature range 80-320 K. The ideality factor increased with decreasing temperature while the barrier height, uncharacteristically (when compared to most semiconductors) too increased with decreasing temperature. The series resistance followed a similar trend, ascribed to a reduction in carrier density with temperature. Furthermore, a linear relationship exists between the barrier height and the ideality factor, confirming the inhomogeneity of the barrier potential. The source of the inhomogeneity is ascribed to localized interface states or traps, perturbing the $\bar{E}$-field below the barrier. A Richardson plot for the Pd/*n*-GaSb SBDs yielded an average barrier height and a Richardson constant smaller than the accepted value, supporting the argument that the barrier is inhomogeneous. The barrier height was found to have a double Gaussian distribution. A plot of the barrier height, $\phi_b\ vs\ 1/2kT$ revealed a double Gaussian distribution for the barrier height with $\phi_{b,\mathrm{mean}}$ assuming values of 0.59 eV ± 0.07 (80-140 K) and 0.25 eV ± 0.12 (140-320 K) respectively.

Acknowledgements

This work is based upon research supported by the SA Research Chairs Initiative of the Department of Science and Technology and National Research Foundation, as well as by the NMMU.

References

[1] P.S. Dutta, H.L. Bhat and V. Kumar, J. Appl. Phys. 81 (1997) 5821-5870.

[2] J. A. Robinson and S.E. Mohney, A low-resistance thermally stable Ohmic contact to n-GaSb, J. Appl. Phys. 98 (2005) 033703.

[3] M. G. Mauk and V. M. Andreev, GaSb-related materials for TPV cells, Semicond. Sci. Technol.. 18 (2003) 191-201.

[4] P. A. Murawala, On the barrier height of Schottky diodes of Au on n-GaSb, Jap. J Appl. Phys. 29 (1990) L2434-L2437.

[5] Z. Y. Liu, D.A. Saulys and T.F. Kuech, Improved characteristics for Au/n-GaSb Schottky contacts through the use of a non-aqueous sulfide-based passivation, Appl. Phys. Lett. 85 (2004) 4391.

[6] D. M. Murape, N. Eassa, J.H. Neethling, R. Betz, E. Coetse, H. C. Swart, J.R. Botha and A. Venter, Treatment for GaSb surfaces using a sulphur blended $(NH_4)_2S/(NH_4)_2SO_4$ solution, Applied Surface Science. 258 (2012) 6753-6758.

[7] O. F Yuksel, Temperature dependence of current-voltage characteristics of Al/p-Si (100) Schottky barrier diodes, Physica B 404 (2009) 1993-1997.

[8] S. S. Naik and V. R. Reddy, Temperature dependency and current transport mechanisms of Pd/V/n-type InP schottky rectifiers, Adv. Mat. Lett. 3 (2012) 188-196.

[9] E. Gur, S. Tuzemen, B. Kılıc and C. Coskun, High-temperature Schottky diode characteristics of bulk ZnO, J. Phys.: Condens. Matter, 19 (2007) 196206.

[10] M. K. Hudait, P. Venkateswarlu and S. B. Krupanidhi, Effects of thin oxide in metal-semiconductor and metal-insulator-semiconductor epi-GaAs Schottky diodes, Solid-State Electronics, 45 (2001) 133-141.

[11] V. Janardhanam, A. A. Kumar, V. R. Reddy and P.N. Reddy, Study of current–voltage–temperature (IVT) and capacitance–voltage–temperature (CVT) characteristics of molybdenum Schottky contacts on n-InP (100), Journal of Alloys and Compounds, 485 (2009) 467-472.

[12] A. Gümüş, A. Türüt and N Yalçin, Temperature dependent barrier characteristics of CrNiCo alloy Schottky contacts on n-type molecular-beam epitaxy GaAs, J. Appl. Phys. 91 (2002) 245.

[13] S. Zeyrek, M. M. Bulbul, S. Altındal, M. C. Baykul and H. Yuzer, The double gaussian distribution of inhomogeneous barrier heights in Al/GaN/p-GaAs (MIS) schottky diodes in wide temperature range, Brazilian Journal of Physics, 38 (2008) 591-597.

[14] Ş. Altındal, S. Karadeniz, N. Tuğluoğlu, A. Tataroğlu, The role of interface states and

series resistance on the I–V and C–V characteristics in Al/SnO2/p-Si Schottky diodes, Solid- State Electronics 47 (2003) 1847-1854.

[15] Chawanda, C. Nyamhere, F. D. Auret, J. M. Nel, W. Mtangi and M. Diale, Current-voltage temperature characteristics of Au/n-Ge (100) Schottky diodes**,** Physica B, 407 (2012) 1570-1573.

[16] S. Chand and J. Kumar, Effect of barrier height distribution on the behaviour of a Schottky diode, J. Appl. Phys. 82 (1997) 5005-5010.

[17] G. Guler, O. Gullu, O.F. Bakkaloglu and A. Turut, Determination of lateral barrier height of identically prepared Ni/n-type Si Schottky barrier diodes by electrodeposition, Physica B, 403 (2008) 2211-2214.

[18] D. E Yildiz, S. Altindal and H. Kanbur, Gaussian distribution of inhomogeneous barrier height in Al/SiO_2/ p-Si Schottky, diodes, J. Appl. Phys. 103 (2008) 124502.

[19] J. H. Werner and H. H. Guttler, Barrier inhomogeneities at Schottky contacts, J. Appl. Phys. 69 (1991) 1522-1533.

[20] D. K. Schroder, Semiconductor material and device characterisation, New Jersey: John Wiley & Sons, 2006. Chapter 3, p137.

[21] M. Jang and Z. Lee, Analysis of Schottky barrier height in small contacts using a thermionic-field emission model**,** ETRI J 24, (2002) 455-461.

[22] M.K. Hudait and S.B. Krupanidhi, Doping dependence of the barrier height and ideality factor of Au/n-GaAs Schottky diodes at low temperatures, Physica B, 307 (2001) 125-137.

[23] J. Verschraegen, M. Burgelman and J. Penndorf, Temperature dependence of the diode ideality factor in $CuInS_2$-on-Cu-tape solar cells, Thin Solid Films, 480-481 (2005) 307-311.

[24] D. Korucu, T.S. Mammadova and S. Özçelik, The role of series resistance on the forward bias current voltage (IV) characteristics in Sn/p-InP (MS) contacts, Journal of Ovonic Research, 4 (2008) 159-164.

[25] A. Turut, M. Saglam, H. Efeoglu, N. Yalcin, M. Yildirim and B. Abay, Interpreting the nonideal reverse bias C-V characteristics and importance of the dependence of Schottky barrier height on applied voltage, Physica B, 205 (1995) 41-50.

[26] M.E. Aydin, K. Akkilic and T. Kilicoglu, The importance of the series resistance in calculating the characteristic parameters of the Schottky contacts, Applied Surface Science, 253 (2006) 1304-1309.

[27] R. Sharma, Temperature dependence of I-V characteristics of Au/n-Si schottky barrier diode, Journal of Electron Devices, 8 (2010) 286-292.

[28] H. Korkut, Y. Yildrim and A. Turut, Thermal annealing effects on I–V–T characteristics of sputtered Cr/n-GaAs diodes, Physica B, 404 (2009) 4039-4044.

[29] F.A. Padovani and R.Stratton, Field and thermionic-field emission in Schottky barriers, Solid State Electron. 9 (1966) 695.

[30] A. Venter, J. R. Botha, V. Wagener and D. M. Murape, Laplace deep level transient spectroscopy of electron traps in epitaxial metalorganic chemical vapor deposition grown *n*-GaSb, J. Appl. Phys. 113 (2013) 024505.

[31] S. Karatas, S. Altindal, A. Turut and M. Cakar, Electrical transport characteristics of Sn/p-Si schottky contacts revealed from I-V-T and C-V-T measurements, Physica B 392 (2007) 43.

[32] A. F. Ozdemir, A. Turut and A. Kokce, The double Gaussian distribution of barrier heights in Au/n-GaAs Schottky diodes from I-V-T characteristics, Semicond. Sci Technol. 21 (2006) 298-302.

[33] C. L. Lin, Y. K. Su, J. R. Chang, S. M. Chen, W. L. Li and D. H. Jaw, Temperature Dependence of barrier height and energy bandgap in Au/n-GaSb Schottky diode, Jpn. J. Appl. Phys. 39 (2000) L400- L401.

[34] W. C Huang, T. C. Lin, C. T. Horng and Y. H. Li, The electrical characteristics of Ni/n-GaSb Schottky diode, Materials Science in Semiconductor Processing 16 (2013) 418–423 8.011).

[35] J. S. Blakemore, Semiconductor Statistics, New York: General Publishing Company, Ltd, 1987. Ch 3, p 258

[36] G. Eftekhari, Effects of sulfur passivation of GaSb on the thermal stability of Al/n-GaSb contacts, Jpn. J. Appl. Phys. 35 (1996) 564-567.

[37] M. E. Aydin, O. Gullu and N. Yildrim, Temperature dependence of current–voltage characteristics of Sn/p-Si Schottky contacts, Physica B, 403 (2008) 131-138.

[38] W. Monch, Barrier heights of real Schottky contacts explained by metal-induced gap states and lateral inhomogeneities, J. Vac. Technol. B 17 (1999) 1867.

[39] S. K. Cheung and N. W. Cheung, Extraction of Schottky diode parameters from forward current-voltage characteristics, Appl. Phys. Lett. 49 (1986) 85-87.